HHS Public Access

NCOA5 deficiency promotes a unique liver protumorigenic microenvironment through p21[WAF1/CIP1] overexpression, which is reversed by metformin

Mark Williams[1,2,*], **Xinhui Liu**[3,4,1,*], **Yueqi Zhang**[1,2], **Jake Reske**[1], **Devika Bahal**[5], **Trevor G. Gohl**[1,8], **Daniel Hollern**[6], **Elliot Ensink**[1], **Matti Kiupel**[7], **Rongcheng Luo**[3], **Rupali Das**[1], **Hua Xiao**[1]

[1]Department of Physiology, Michigan State University, East Lansing, Michigan 48824

[2]Cellular and Molecular biology Program, Michigan State University, East Lansing, Michigan 48824

[3]Cancer Center, Southern Medical University, Guangzhou, Guangdong, China 510315

[4]Integrated hospital of Traditional Chinese Medicine, Southern Medical University, Guangzhou, Guangdong, China 510315

[5]Comparative Medicine and Integrative Biology Program, Michigan State University, East Lansing, Michigan 48824

[6]Lineberger Comprehensive Cancer Center, The University of North Carolina Chapel Hill, NC 27599

[7]Department of Pathobiology and Diagnostic Investigation, Michigan State University, East Lansing, Michigan 48910

[8]Current affiliation: College of Osteopathic Medicine, Michigan State University, East Lansing, Michigan 48824

Abstract

Prevention and treatment options for hepatocellular carcinoma (HCC) are presently limited, underscoring the necessity for further elucidating molecular mechanisms underlying HCC development and identifying new prevention and therapeutic targets. Here, we demonstrate a unique protumorigenic niche in the livers of *Ncoa5*^{+/−} mouse model of HCC, which is characterized by altered expression of a subset of genes including p21[WAF1/CIP1] and proinflammatory cytokine genes, increased putative hepatic progenitors, and expansions of activated and tissue-resident memory (TRM) CD8+ T lymphocytes, myeloid-derived suppressor cells (MDSCs) and alternatively activated M2 macrophages. Importantly, prophylactic metformin

Correspondence: Hua Xiao, M.D., Ph.D., Professor of Department of Physiology, Michigan State University, 3193 Biomedical and Physical Sciences Building, East Lansing, MI 48824-3320, Phone: 517-884-5127; Fax: 517-355-5125; xiaoh@msu.edu.
*These authors contributed equally to this work.

treatment reversed these characteristics including aberrant p21$^{WAF1/CIP1}$ expression and subsequently reduced HCC incidence in *Ncoa5*$^{+/-}$ male mice. Heterozygous deletion of the p21$^{WAF1/CIP1}$ gene alleviated the key features associated with the protumorigenic niche in the livers of *Ncoa5*$^{+/-}$ male mice. Moreover, transcriptomic analysis reveals that preneoplastic livers of *Ncoa5*$^{+/-}$ mice are similar to the livers of non-alcoholic steatohepatitis patients as well as the adjacent noncancerous liver tissues of a subset of HCC patients with a relatively poor prognosis. Together, our results suggest that p21$^{WAF1/CIP1}$ overexpression is essential in the development of pro-tumorigenic microenvironment induced by NCOA5 deficiency and metformin prevents HCC development via alleviating p21$^{WAF1/CIP1}$ overexpression and protumorigenic microenvironment.

Keywords

Introduction

Hepatocellular carcinoma (HCC) accounts for the majority of primary liver cancer occurrences and is currently the second leading cause of cancer-related death worldwide [1, 2]. Although early stage HCC can be potentially alleviated by curative treatments such as surgical resection, liver transplantation and local ablation, intrahepatic reappearance of HCC often occurs in patients within five years due to both metastatic recurrence and newly-developed primary HCC [2, 3]. Currently, systemic options for the prevention and treatment of this disease are limited, underscoring the need for discovery of new therapeutic targets and prevention strategies as well as biomarkers for patient stratification [3, 4].

HCC development is a complex and multistep process caused by diverse risk factors including chronic hepatitis viral infection, alcohol consumption, and metabolic diseases such as obesity, non-alcoholic steatohepatitis (NASH) and diabetes. Many of these risk factors are known to induce sustained inflammatory damage, hepatocyte necrosis and regeneration that result in the formation of a pro-tumorigenic hepatic microenvironment characterized by molecular and cellular changes in both the parenchymal and non-parenchymal cells, ultimately leading to HCC occurrence. In the past decades, significant advances have been made to uncover various cellular factors, oncogenic drivers and pathogenic pathways that contribute to the initiation and progression of HCC [3, 4]. In particular, inflammatory cytokines produced by hepatic infiltrating macrophages, and resident Kupffer cells have been demonstrated to promote development of NASH and HCC through activation of NF-kB and STAT3 signaling pathways in diethylnitrosamine (DEN) or high-fat diet-induced and genetically-engineered mouse models of HCC [5–7]. Despite these findings, the molecular basis of HCC development remains to be fully elucidated.

We previously reported that male mice carrying a heterozygous deletion of the *Ncoa5* gene exhibited glucose intolerance, chronic hepatic inflammation and a high incidence of HCC [8, 9]. In this study, we aimed to identify cellular molecules and pathways in precancerous livers that are essential for HCC development. Using this *Ncoa5*$^{+/-}$ mouse model of HCC, we investigated alterations in transcriptomic profiles, signaling pathways and cellular targets

in preneoplastic livers as well as responses to prophylactic metformin treatment that has been implicated in the prevention of HCC development in mice and humans [10–12]. Our work demonstrated that aberrant expression of p21^WAF1/CIP1, a potent cyclin-dependent kinase inhibitor, is required for the formation of a hepatic protumorigenic microenvironment in hepatocarcinogenesis, which can be reversed by prophylactic metformin treatment.

Materials and methods

Genetically Engineered Model of Hepatocellular Carcinoma and Treatments

BALB/c *Ncoa5*^+/− female mice [9] were backcrossed with C57BL/6J males for 7 generations to produce C57BL/6J *Ncoa5*^+/− male mice that were used. All mice were housed in Optimice cages at Michigan State University animal facility and fed standard rodent diet *ad libitum*. The numbers of mice for the tumor incidence experiment were chosen to ensure approximately 80% power (0.05 level of significance, two-side test) to detect at least a 30% difference in HCC development. Male mice were purely randomly allocated to metformin treated or untreated group. Female mice were excluded because only *Ncoa5*^+/− male mice were previously reported to develop HCC in 10–18 months and human HCC predominantly develop in men [9]. The investigator was not blinded to the group allocation during the experiment and assessing the outcome. Mice in metformin experiments received metformin (PHR1084, Sigma Aldrich) dissolved in drinking water at a dosage of approximately 250mg/kg/day from 8 weeks until 48 weeks of age. All experimental procedures on mice were approved by the Michigan State University Institutional Animal Care and Use Committee.

Quantitative PCR, RNA-Seq and Transcriptomic Analyses of Mouse Liver Tissues and Human HCC Samples

Quantitative PCR was performed as described previously [9]. Oligonucleotides for the primers are described in Table S1. Preparation of liver RNA samples, high throughput RNA-Seq analysis and further human HCC and non-alcoholic fatty liver disease samples and analyses, the 39-week-old *Ncoa5*^+/− liver gene set (containing 107 genes) and Metformin reversal gene set (containing 28 genes) and score were described in supplementary materials and methods.

Serological Analyses

Mouse serum Alanine transaminase (ALT) was measured with kit #700260 from Cayman chemical (Ann Arbor, MI).

Tissue Histology, Immunohistochemistry (IHC) and Immunofluorescence

Hematoxylin and eosin staining of tissue sections and IHC were performed as previously described [9]. Pathologic analysis was carried out by a board-certified veterinary pathologist, M.K. Quantification of EPCAM-positive, Keratin 19 (KRT-19)-positive, MAC-2-postive, and the IHC labeling score of p21^WAF1/CIP1 and p16^INK4A were determined in five random fields per slide. Immunofluorescent labeling was performed as described previously [13]. 0.1% Sudan black B (3545–12, Sigma) in 70% ethanol was used to reduce the autofluorescence of the tissue.

Flow Cytometry

Antibodies used in the study was described in the Table S2. Data were collected on a BD LSRII flow cytometer (BD Biosciences, San Jose, CA) and analyzed using FlowJo software (Tree Star, Ashland, OR).

Statistics

All results were presented as means± SD or ±SEM as indicated. The differences between groups were analyzed with one-way or two-way ANOVA, Student's *t*-test or Mann–Whitney U test with two-tailed. The overall survival (OS) and disease-free survival (DFS) were analysis by Log-Rank test using GraphPad Prism 7. ** $P < 0.01$,* $P < 0.05$, NS = not significant.

Availability of data and materials

The RNA sequencing data have been deposited in NCBI's Gene Expression Omnibus and are accessible through GEO Series accession number GSE110524 (https://www.ncbi.nlm.nih.gov/geo/query/acc.cgi?acc=GSE110524). All other data that support the findings of this study are available within the article and its supplementary information files or from the corresponding author upon reasonable request.

Results

Dysregulation of *Cdkn1a*/p21^WAF1/CIP1 and Proinflammatory Cytokine Genes in p53 and Inflammatory Response Pathways in *Ncoa5*^+/− Male Mouse Livers

We previously reported that NCOA5 haplo-insufficiency enhances expression of IL-6 and TNF-α in Kupffer cells, which in turn promotes hepatic inflammation, steatosis and HCC development [9]. To gain further insight into the molecular mechanisms that contribute to HCC development, differentially-expressed genes between early preneoplastic livers of *Ncoa5*^+/− and *Ncoa5*^+/+ male mice at 20 weeks of age were identified through high throughput RNA-Seq and differential gene expression analyses (Fig. 1A, Supplementary Fig. S1A and Table S3A). Of note, many of these genes were known as the downstream targets of NF-kB, which are involved in inflammatory processes implicated in HCC development. Furthermore, 18 of these mouse genes have human homologs that were significantly correlated with NCOA5 expression in human HCC and adjacent-tissue specimens, indicating similarities in the effect of NCOA5 deficiency between mice and humans (Fig. 1B). Particularly, two canonical p53 target genes, namely *Cdkn1a*/p21^WAF1/CIP1 [14] and *Gadd45β*, were upregulated in livers of *Ncoa5*^+/− male mice. Consistently, expression of 37 KEGG gene sets in *Ncoa5*^+/− mouse livers were altered and include p53, NF-kB, and MAPK signaling pathways (Supplementary Fig. S1B and Table S4A and 4B). RNA-Seq was also carried out in livers of 39-week-old *Ncoa5*^+/− (n=5) and *Ncoa5*^+/+ male mice (n=4) at a later preneoplastic stage of hepatocarcinogenesis (Supplementary Table S5). Twenty genes with significantly altered expression (log2 fold change>1 and a similar direction in expression change) were shared between 20- and 39-week results and include *Cdkn1a*/p21^WAF1/CIP1 (Fig. 1C). p53 signaling pathway was also persistently up-regulated in the 39-week-old cohort (Supplementary Fig. S1B and Table S6).

The mRNA levels of p21$^{WAF1/CIP1}$ and *Gadd45β* were confirmed to be elevated in the livers of *Ncoa5*$^{+/-}$ male mice at the ages of 8, 20 and 39 weeks (Fig. 1D and Supplementary Fig. S2). In contrast, expression of *Cdkn2a*/p16^{INK4A}, another cell cycle kinase inhibitor, was not significantly changed (Supplementary Fig. S3A–C). IHC staining revealed that increased expression of p21$^{WAF1/CIP1}$ was predominantly localized to the cytoplasm of hepatocytes in the livers of *Ncoa5*$^{+/-}$ male mice (Fig. 1E and Supplementary Fig. S3D). Elevation of p21$^{WAF1/CIP1}$ mRNA was accompanied by increased expression of several cytokines and chemokines including IL-6 and CCL2 and in the livers of *Ncoa5*$^{+/-}$ male mice at both ages of 20 and 39 weeks (Fig. 1F). Since these factors may influence hepatic progenitor cell (HPC) differentiation and proliferation in early cancer-initiating events [4, 15–17], hepatic cells were examined for expression of EPCAM and KRT-19, two biomarkers for hepatic progenitor cells and cholangiocytes. As expected, EPCAM and KRT-19 positive small epithelial cells with an oval-shaped nucleus and a limited amount of cytoplasm, were significantly increased in the livers of *Ncoa5*$^{+/-}$ male mice (Fig. 1G and Supplementary Fig.S4), indicating an increased putative HPCs in the livers of *Ncoa5*$^{+/-}$ male mice. In addition, qPCR analysis showed that NCOA5 knockdown could augment genotoxic agent camptothecin (CPT) or IL-6-induced p21$^{WAF1/CIP1}$ expression in human HCC HepG2 cells (Supplementary Fig. S5). Together, these data suggest that upregulation of p21$^{WAF1/CIP1}$ in hepatocytes is possibly associated with the development of protumorigenic microenvironment in livers of *Ncoa5*$^{+/-}$ male mice.

Intrahepatic CD8+ T cells, MDSCs and M2 Macrophages are Specifically Increased in the Protumerigenic Liver of the *Ncoa5*$^{+/-}$ Male Mice

Since many risk factors of HCC provoke an inflammatory response characterized by hepatic infiltration of lymphocytes and macrophages, we investigated the immune landscape of the protumorigenic livers as well as the spleens and thymi of the *Ncoa5*$^{+/-}$ male mice. As expected in chronic inflammatory livers, the total number of intrahepatic mononuclear cells were significantly increased in the livers of *Ncoa5*$^{+/-}$ mice, while the total number of thymocytes and splenocytes were comparable in age-matched *Ncoa5*$^{+/+}$ and *Ncoa5*$^{+/-}$ mice (Supplementary Fig. S6). Flow cytometric analysis revealed a significant increase in the frequency of total T cells (TCRβ+), which was associated with a dramatic increase in CD8+ T cells and proportional decrease in the incidence of CD4+ T cells (Fig. 2A and Supplementary Fig. S7A). Furthermore, while the frequency of B cells was decreased significantly, incidence of natural killer (NK) cells remained unaffected (Supplementary Fig. S5B). However, the absolute numbers of all these lymphocytic populations were significantly higher in the precancerous livers of the *Ncoa5*$^{+/-}$ mice (Fig. 2B and Supplementary Fig. S7B). In contrast, no significant differences in the incidences and cell numbers of splenic T (CD4+ or CD8+), B, and NK cells were detected between these two group animals (Supplementary Fig. S8).

Chronic inflammation results in phenotypic switch in macrophage populations from M1 to tumor-promoting and immunosuppressive M2 phenotype and changes of T cell populations from activation to exhaustion, as well as increase of immune-suppressive cells such as myeloid-derived suppressor cells (MDSCs), which evades immune surveillance and contributes to the development of protumorigenic environment [18]. We therefore carried

out further phenotypic evaluation of the CD4+ and CD8+ T cell compartments as well as macrophage populations. Strikingly, proportion and number of activated (CD62L– CD44+) and tissue-resident memory (T_{RM}, CD69+CD103+) CD8+ T cells were significantly augmented in the livers of $Ncoa5^{+/-}$ mice (Fig. 2C, 2D and Supplementary Fig. S9A). The proportion and number of T_{RM} CD4+ T cells were also significantly increased in the livers of these animals, while only the number of activated CD4+ T cells was significantly increased (Supplementary Fig. S9B and S9C). Consistent with the previous observation of the increased total number of hepatic macrophages [9], significant increases of several immunosuppressive cell types including MDSCs (CD11b+F4/80+Gr-1+), macrophages (CD11b+F4/80+CD14+) and M2 macrophages (CD14+F4/80+CD206+) were observed specifically in the livers of $Ncoa5^{+/-}$ male mice (Fig. 3). Collectively, these results suggest that NCOA5 haploinsufficiency results in a protumorigenic environment containing increased intrahepatic populations of activated and T_{RM} CD8+ T cells and immunosuppressive cells including MDSCs, macrophages and M2 macrophages.

Metformin Alleviates the Characteristics of Hepatic Protumorigenic Microenvironment and the Incidence of HCC in $Ncoa5^{+/-}$ Male Mice

Previous studies suggest that metformin treatment can inhibit HCC development in diethylnitrosamine (DEN) or high fat diet induced animal models of HCC [10–12]. In order to establish a causal link between dysregulated gene expression and HCC development in $Ncoa5^{+/-}$ male mice, we examined whether metformin inhibits HCC development in $Ncoa5^{+/-}$ male mice. A cohort of $Ncoa5^{+/-}$ and $Ncoa5^{+/+}$ C57BL/6 male mice were treated with metformin which started at 8 weeks of age and terminated at 48 weeks of age and then observed for development of preneoplastic lesions and HCC until 78 weeks of age (Fig. 4A). A dramatic reduction in the incidence of HCC was observed in male $Ncoa5^{+/-}$ mice treated with metformin versus untreated $Ncoa5^{+/-}$ male mice (Fig. 4B), demonstrating that metformin treatment reduces the incidence of HCC. Furthermore, the number of Ki67-positive hepatocytes in metformin-treated $Ncoa5^{+/-}$ male mice were significantly lower than untreated $Ncoa5^{+/-}$ male mice and similar to that of wild type mice, suggesting a reduction in hepatic proliferation induced by metformin treatment (Fig. 4C and Supplementary Fig. S10). Moreover, serum ALT levels, reflecting liver damage, were significantly reduced by metformin in $Ncoa5^{+/-}$ male mice, while markedly increased in $Ncoa5^{+/-}$ male mice as compared to $Ncoa5^{+/+}$ male mice (Fig. 4D).

We next investigated the effect of metformin treatment on the homeostasis of immune cell populations. We observed that metformin did not alter the cellularity of the thymi or the spleens of $Ncoa5^{+/+}$ or $Ncoa5^{+/-}$ male mice (Supplementary Fig. S11). However, it significantly decreased the total intrahepatic mononuclear cell counts in $Ncoa5^{+/-}$ but not $Ncoa5^{+/+}$ male mice (Supplementary Fig. S11). Consistently, total numbers of intrahepatic CD4+ and CD8+ T lymphocytes (Fig. 4E and S12) as well as activated and T_{RM} subsets of CD8+ T cells (Fig. 4F, Supplementary Fig.S13 and S14A) were significantly reduced in metformin-treated $Ncoa5^{+/-}$ male mice. Similarly, metformin-treated $Ncoa5^{+/-}$ male mice also displayed significantly reduced total intrahepatic myeloid cell populations and incidence of intrahepatic MDSCs and M2 macrophages (Fig. 4G). The numbers of intrahepatic macrophages and M2 macrophages tended to decrease in metformin-treated

$Ncoa5^{+/-}$ male mice (Supplementary Fig. S14B). These results suggest that prophylactic treatment with metformin can ameliorate chronic inflammatory response of intrahepatic immune cells in a precancerous liver.

Metformin Reduces Aberrant p21[WAF1/CIP1] Expression and Enrichment of Exhausted CD8+ T Lymphocyte Gene Signatures in Livers of $Ncoa5^{+/-}$ Male Mice

To identify potential molecular mechanisms mediating the action of metformin in the prevention of HCC development in $Ncoa5^{+/-}$ mice, RNA-Seq and differential gene expression analyses on livers of $Ncoa5^{+/-}$ and $Ncoa5^{+/+}$ mice with or without metformin treatment revealed that the mRNA levels of p21[WAF1/CIP1] and 45 other genes were significantly reversed with metformin treatment (Fig. 5A). Several pathways, including p53 and primary immunodeficiency pathways, had been upregulated in $Ncoa5$ mice, displayed a reduced trend with metformin treatment to be more like $Ncoa5$ mice (Fig. 5B). In agreement with the results from the RNA-Seq analysis, p21[WAF1/CIP1] mRNA levels were confirmed to be reduced by 43% with metformin treatment in $Ncoa5^{+/-}$ mice (Fig. 5C). Consistent with that, the IHC labeling score was also reduced, reflecting the reduced number of cytoplasmic p21[WAF1/CIP1]-positive hepatocytes by metformin (Fig. 5D). Additionally, HPC-like cells positively stained by EPCAM and KRT-19 antibodies were dramatically decreased in metformin treated $Ncoa5^{+/-}$ mice compared to the untreated $Ncoa5^{+/-}$ group (Fig. 5E). These data indicate that metformin treatment reduces expression of dysregulated genes including p21[WAF1/CIP] overexpression and expansion of putative HPCs in livers of $Ncoa5^{+/-}$ male mice.

Consistent with the observations of the phenotypic changes in CD8+ T cell populations in the livers of $Ncoa5^{+/-}$ male mice, enrichment of two T-cell exhaustion gene signatures [19, 20] were increased in the liver of $Ncoa5^{+/-}$ male mice compared to control livers, but were significantly reduced in the liver of metformin-treated $Ncoa5^{+/-}$ mice (Figure S15A and B). In contrast, genes typically expressed in T-effector cells as described previously [21] was down-regulated in the livers of $Ncoa5^{+/-}$ male mice, but was increased by metformin treatment (Supplementary Fig. S15C), suggesting a reduction of inflammation such that T-cells are not driven into exhausted states. In agreement with previous findings on the action of metformin on Stat3 signaling pathway [22, 23], enrichment of Stat3 signaling pathway gene signatures [24] was elevated in the livers of $Ncoa5^{+/-}$ male mice, but was significantly reduced by metformin (Supplementary Fig. S15D). Taken together, these results suggest that the inhibition of HCC development by the prophylactic metformin treatment is mediated by recoiling the protumorigenic niche in the livers of $Ncoa5^{+/-}$ male mice.

Heterozygous Deletion of the p21[WAF1/CIP1] Gene Inhibits the Formation of a Protumorigenic Niche in the Livers of $Ncoa5^{+/-}$ Male Mice.

To determine the role of p21[WAF1/CIP1] overexpression in this protumorigenic niche, we examined the effect of decreased p21[WAF1/CIP1] expression on the aforementioned characteristics of the protumorigenic niche by comparing between the livers from $Ncoa5^{+/-}$ and $Ncoa5^{+/-}p21^{+/-}$ male mice for avoiding the complications caused by complete p21[WAF1/CIP1] ablation. The mRNA levels of 14 early up-regulated genes, which were identified in the livers of $Ncoa5^{+/-}$ male mice at 20 weeks of age (Supplementary Fig.S1),

were measured. Reduced mRNA expression of *Cdkn1a*/p21$^{WAF1/CIP1}$ was accompanied by a significant decrease (2 genes) or trending decrease (10 genes) in mRNA levels of measured genes in livers of *Ncoa5*$^{+/−}$*p21*$^{+/−}$ double mutant mice compared to livers of *Ncoa5*$^{+/−}$ mice (Fig. 6A). Moreover, immunohistochemical analysis revealed that the numbers of cytoplasmic p21$^{WAF1/CIP1}$-positive hepatocytes, macrophages and putative HPCs were also significantly reduced in livers of *Ncoa5*$^{+/−}$*p21*$^{+/−}$ double mutant male mice compared to *Ncoa5*$^{+/−}$ mouse livers (Fig. 6B). These results further support our notion that increased p21$^{WAF1/CIP1}$ expression plays a critical role in the development of a hepatic protumorigenic niche.

Expression of CDKN1A/p21$^{WAF1/CIP1}$ and NCOA5 Gene Sets are Associated with Human HCC Patient Survival

To assess relevance of our findings in precancerous mouse livers to human HCCs, non-cancerous HCC-adjacent tissue samples from a cohort of 214 human patients [25] were analyzed for Hallmark gene set enrichment and then classified by unsupervised hierarchical clustering. Based on similarities in gene set enrichment, this cohort of patients was classified into three major clusters (Fig.7A). Similar to the observations in the livers of *Ncoa5*$^{+/−}$ mice, several pathways, including p53 and inflammatory pathways were positively enriched in a subset (Cluster C, n=71, 33%, Fig. 7A). Notably, the enrichments of the NCOA5 gene set (containing 107 genes, identified in 39-week-old *Ncoa5*$^{+/−}$ livers) and the metformin reversal gene set (containing 28 genes), which both include CDKN1A/p21$^{WAF1/CIP1}$ gene (Supplementary Table S7) were significantly different in the three clusters, and we identified a subset (cluster C) of patients with precancerous states similar to our murine cohort. Interestingly, patients in cluster A displayed a high enrichment of the metformin reversal gene set compared to patients in cluster C, indicating that the hepatic gene expression profile in those patients was similar to that of *Ncoa5*$^{+/−}$ mouse precancerous livers after treatment with metformin. Using the same analysis on another cohort of 168 patients [26], three major clusters of patients were also classified and similar correlations of patient clusters with NCOA5 gene set or metformin reversal gene set enrichments were observed (Supplementary Fig. S16). Unsupervised hierarchical clustering of enrichment of hallmark gene sets on both HCC and their adjacent non-cancerous tissues in cluster C patients identified two major clusters that displayed profound differences in enrichment of aforementioned Hallmark gene sets between them (Supplementary Fig. S17). Of note, high expression of CDKN1A/p21$^{WAF1/CIP1}$, enrichments of p53 pathway signature and inflammatory response gene sets were associated with the cluster containing the majority of noncancerous tissues (Supplementary Fig. S17). Furthermore, a significant negative regression coefficient between CDKN1A/p21$^{WAF1/CIP1}$ expression and the metformin reversal gene set enrichment was determined, which was consistent with what was seen in the liver of *Ncoa5*$^{+/−}$ male mice treated with metformin (Fig. 7B). Thus, the precancerous niche in the livers of *Ncoa5*$^{+/−}$ mice may mimic noncancerous liver tissues with an upregulated CDKN1A/p21$^{WAF1/CIP1}$ expression and p53 and inflammatory response pathways in a subset (33%) of human HCCs. In support of our observations, cluster C patients also displayed a strong association with a 12-chemokine gene ectopic lymphoid-like structure (ELS) set (Fig. 7A), which was previously reported to be enriched in the cirrhotic liver tissues of surgically-treated HCC patients associated with poorer OS and higher late recurrence [17].

To determine the clinical significance of our findings, clinicopathologic features of the patients between cluster C and other clusters were compared. Of specific interest was that patients in cluster C had a significant association with higher serum ALT level, advanced cancer stages and poorer predicted survival (Table S8). Consistently, patients in cluster C had a significantly shorter Overall Survival (OS) and Disease Free Survival (DFS) (Fig. 7C). Moreover, we assessed the expression of metformin reversal genes in the adjacent noncancerous tissues by using a previously-described scoring method derived from principal component analysis [27]. The scoring result resembled the expression of the metformin reversal gene set across this patient cohort, and was significantly different in the aforementioned three clusters (Fig. 7A). Strikingly, patients with a low metformin reversal gene score had a considerably shorter OS and DFS compared to those with a high score (Fig. 7D).

To further explore the relevance of our findings to human non-alcoholic steatohepatitis (NASH)-driven HCC, we assessed expression of the NCOA5 gene set and the metformin reversal gene sets in liver tissues from NASH, simple steatosis and healthy individuals [28]. The NCOA5 gene set was significantly enriched in liver tissues from NASH and simple steatosis patients compared to liver tissues from healthy people (Fig. 7E). In addition, NASH patients had a low metformin reversal gene score compared to patients with simple steatosis (Fig. 7F). Collectively, these results suggest that a precancerous niche containing p21$^{WAF1/CIP1}$ overexpression and enrichment of NCOA5 gene set, as well as a low metformin reversal gene score, may impact the initiation and progression of HCC. Likewise, HCC patients with such a niche have a poor prognosis.

Discussion

In this study, we uncovered altered transcriptomic profiles, signaling pathways and cellular targets in the early and late preneoplastic stages of mouse livers in hepatocarcinogenesis, and identified hepatic responses to metformin treatment. In particular, our results support that p21$^{WAF1/CIP1}$ overexpression is essential for the formation of a unique tumor-prone microenvironment in hepatocarcinogenesis. Moreover, metformin treatment can inhibit key features associated with the protumorigenic niche, leading to a significant reduction of HCC incidence in $Ncoa5^{+/-}$ male mice. Thus, our results provide not only a molecular mechanism underlying the development of hepatic pro-cancerous microenvironment but also insight into molecular mechanisms that mediate the cancer-preventive actions by metformin. Furthermore, our study suggests that a subset of HCC patients, having gene expression changes similar to the precancerous livers of $Ncoa5^{+/-}$ male mice in the adjacent noncancerous liver tissues, may have a high risk of HCC recurrence and worse survival rates. Given the fact that there is an urgent need for molecular classification of both the tumor and its microenvironment to assist more effective clinical decision making and treatment selection for HCC patients [4], our findings open a possibility to stratify HCC patients using the NCOA5 gene set and metformin reversal gene score for receiving adjuvant treatment with metformin.

The cellular functions of p21$^{WAF1/CIP1}$ are known to be largely dependent on its subcellular localization and interactions with other cellular proteins [29]. Even though p21$^{WAF1/CIP1}$

acts as a tumor suppressor when localized to the nuclei, it also acts as an oncoprotein in the context of certain cellular changes to promote tumorigenesis [29–32]. Increased hepatic p21$^{WAF1/CIP1}$ expression has been reported to be correlated with hepatic pretumorigenic lesions such as chronic hepatic injuries and non-alcoholic fatty liver disease/NASH in various animal models of hepatic steatosis and human liver specimens from patients [33, 34]. Indeed, transgenic mice with hepatocyte-specific overexpression of p21$^{WAF1/CIP1}$ exhibited increased numbers of hepatic oval cells, which are bipotential progenitors, and formation of nodular foci of hepatocytes in the liver [35]. Moreover, the cytoplasmic p21$^{WAF1/CIP1}$ expression in hepatocytes was previously reported to positively correlate with HCC development in transgenic CD-1 mice expressing the hepatitis B virus X gene [36]. Nevertheless, there have been opposite findings as to whether p21$^{WAF1/CIP1}$ promotes or inhibits HCC development in mouse models of HCC. Homozygous deletion of p21$^{WAF1/CIP1}$ was shown to impair HPC proliferation and delay HCC formation in the Mdr2 knockout mouse model of HCC that has NF-kB signaling activation in hepatocytes [37]. In contrast, homozygous deletion of p21$^{WAF1/CIP1}$ increased cellular DNA damage and promoted HCC development in the NEMO ^{hepa} mouse model of HCC that lacks NF-kB signaling activation in hepatocytes [38]. Thus, it was proposed that the oncogenic role of p21$^{WAF1/CIP1}$ in hepatocarcinogenesis may depend on the presence of NF-kB signaling activation. Our work extends this view by suggesting that p21$^{WAF1/CIP1}$ overexpression is required for the formation of cancer-prone microenvironment through altering expression of a set of specific genes and increased immune cell infiltrations in the *Ncoa5$^{+/−}$* mouse model of HCC, which also contains activated NF-kB signaling in the liver [9]. In keeping with the currently understood regulation of p21$^{WAF1/CIP1}$ expression [39], we speculate that NCOA5 deficiency may increases p21$^{WAF1/CIP1}$ expression through enhancing p53 and NF-kB-mediated transcriptional activation in hepatocytes in response to the proinflammtory and stressed hepatic microenvironment in *Ncoa5$^{+/−}$* male mice. In support of this scenario, we have observed that myeloid-specific deletion of *Ncoa5* gene significantly increased p21 mRNA and protein levels in livers of male mice at age of 10 months (Zhang and Xiao, unpublished results). Moreover, we show that NCOA5 knockdown could augment CPT- or IL-6-induced p21$^{WAF1/CIP1}$ expression in HepG2 cells (supplementary Fig. S5). However, we cannot rule out a possibility that NCOA5 deficiency reduces its binding to the NF-kb site of p21 promoter [39], thereby relieving its suppression of p21$^{WAF1/CIP1}$ transcription since NCOA5 was previously reported to negatively regulate IL-6 transcription via a direct binding of NCOA5 to the NF-kB site of *IL-6* promoter [9].

Epidemiological studies showed that individuals with type-2 diabetes treated with metformin had a reduced risk of both HCC incidence and mortality [40–42]. Distinctive mechanisms including activation of AMP-activated protein kinase (AMPK) or inhibition of AMPK independent pathways, such as suppression of AMPK independent de novo lipid synthesis, were suggested by previous studies on several preclinical cancer models [10–12, 43–46]. Metformin was previously shown to inhibit high glucose-induced p21$^{WAF1/CIP1}$ expression in human embryonic kidney HEK293 cells via AMPK activation [47] and decrease p21$^{WAF1/CIP1}$ protein levels and expression of inflammatory cytokines associated with senescence in different human fibroblasts via DICER1 upregulation[48]. Consistent with the previous observations, we have observed that metformin treatment reversed the aberrant

expression of a set of genes including p21$^{WAF1/CIP1}$ gene and the activation of cancer-related pathways in *Ncoa5$^{+/-}$* mouse liver, although it is not clear whether metformin directly augments the function of NCOA5. Moreover, genetic inhibition of p21$^{WAF1/CIP1}$ expression also resulted in reduced expression of inflammatory responsive genes, reduced infiltration of macrophages and reduced proliferation of putative HPCs in *Ncoa5$^{+/-}$* mouse livers. It is conceivable that prophylactic metformin treatment might upregulate AMPK- and DICER1-mediated pathways to inhibit expression of p21$^{WAF1/CIP1}$ as well as to alter expression of other genes important in hepatic protumorigenic environment induced by NCOA5 deficiency. Thus, we propose that inhibition of p21$^{WAF1/CIP1}$ expression is at least one of metformin-mediated actions to inhibit hepatic protumorigenic environment and subsequently reduce HCC incidence.

Chronic inflammation contributes tumorigenesis through multiple mechanisms, one of which is the development of an immune suppressive environment. The preneoplastic livers of *Ncoa5$^{+/-}$* male mice apparently retain a unique immune environment containing increased populations in intrahepatic activated and T_{RM} CD8+ T cells accompanied with accumulation of immunosuppressive cells such as MDSCs and M2 macrophages. Recent studies have suggested that infiltrated activated and memory CD8+ T cells play an important role of in the surveillance of cancer progression, and their presence in HCCs has positive prognostic and therapeutic value [49]. Despite this important finding, the continuous growth and frequent recurrence of HCCs as well as their poor prognosis yet reflect the failure of effective immune control of cancer progression. This is perhaps due to several immunosuppressive mechanisms within the protumorigenic microenvironment, one of which is likely to be involved in the exhaustion and subsequent dysfunction of CD8+ T cells [50]. The observation of the enrichment of exhausted CD8+ [20] and Stat3 signaling gene signatures [24] in the precancerous liver of *Ncoa5$^{+/-}$* male mice at the age of 39 weeks implied that these activated and T_{RM} CD8+ T cells might be exhausted by a long-term chronic inflammation. Nevertheless, our studies suggest that metformin treatment is able to reduce hepatic infiltration of CD8+ T cells and macrophages and enrichment of exhausted CD8+ and Stat3 signaling gene signatures in the liver of *Ncoa5$^{+/-}$* male mice. In particular support of our findings, induction of CD8+ T cell exhaustion by inflammation-induced IgA+ cells was shown to be involved in liver tumor development [51]. Moreover, several lines of evidence support the effect of metformin on CD8+ T cell proliferation and differentiation [52]. In a study with multiple types of established cancers in BALB/c mice, metformin treatment was shown to result in CD8+T cell-dependent tumor rejection, which was associated with the inhibition of the immune exhaustion of tumor infiltrating CD8+ lymphocytes[50]. Thus, in addition to the mechanistic insights into actions of metformin, our data could be valuable in supporting that metformin treatment may be beneficial in reversing the immune suppressive and CD8+ T cell exhausted tumor microenvironment for HCC patients.

In summary, our work demonstrates that a unique protumorigenic niche promotes HCC development in *Ncoa5$^{+/-}$* male mice and metformin is able to disrupt this niche and prevent HCC development. The results also implicate that a subset of HCC patients might potentially be stratified by metformin reversal scores for adjuvant metformin therapy after HCC resection. Our findings highlight the importance of targeting the precancerous

microenvironment for the prognosis, prevention and treatment of HCC, and p21$^{WAF1/CIP1}$ is a potential target for chemopreventive and therapeutic strategies against HCC development.

Supplementary Material

Refer to Web version on PubMed Central for supplementary material.

Acknowledgements

References

1. Torre LA, Siegel RL, Ward EM, Jemal A. Global Cancer Incidence and Mortality Rates and Trends--An Update. Cancer Epidemiol Biomarkers Prev 2016; 25: 16–27. [PubMed: 26667886]

2. Gerbes A, Zoulim F, Tilg H, Dufour JF, Bruix J, Paradis V et al. Gut roundtable meeting paper: selected recent advances in hepatocellular carcinoma. Gut 2018; 67: 380–388. [PubMed: 29150490]

3. Llovet JM, Zucman-Rossi J, Pikarsky E, Sangro B, Schwartz M, Sherman M et al. Hepatocellular carcinoma. Nat Rev Dis Primers 2016; 2: 16018. [PubMed: 27158749]

4. Sia D, Jiao Y, Martinez-Quetglas I, Kuchuk O, Villacorta-Martin C, Castro de Moura M et al. Identification of an Immune-specific Class of Hepatocellular Carcinoma, Based on Molecular Features. Gastroenterology 2017; 153: 812–826. [PubMed: 28624577]

5. Nakagawa H, Maeda S. Inflammation- and stress-related signaling pathways in hepatocarcinogenesis. World J Gastroenterol (Editorial Research Support, Non-U.S. Gov't Review) 2012; 18: 4071–4081. [PubMed: 22919237]

6. Naugler WE, Sakurai T, Kim S, Maeda S, Kim K, Elsharkawy AM et al. Gender disparity in liver cancer due to sex differences in MyD88-dependent IL-6 production. Science 2007; 317: 121–124. [PubMed: 17615358]

7. Park EJ, Lee JH, Yu GY, He G, Ali SR, Holzer RG et al. Dietary and genetic obesity promote liver inflammation and tumorigenesis by enhancing IL-6 and TNF expression. Cell (Research Support, N.I.H., Extramural Research Support, Non-U.S. Gov't) 2010; 140: 197–208. [PubMed: 20141834]

8. Dhar D, Seki E, Karin M. NCOA5, IL-6, type 2 diabetes, and HCC: The deadly quartet. Cell Metab (Comment Research Support, N.I.H., Extramural Research Support, Non-U.S. Gov't) 2014; 19: 6–7. [PubMed: 24411937]

9. Gao S, Li A, Liu F, Chen F, Williams M, Zhang C et al. NCOA5 haploinsufficiency results in glucose intolerance and subsequent hepatocellular carcinoma. Cancer Cell 2013; 24: 725–737. [PubMed: 24332041]

10. Bhalla K, Hwang BJ, Dewi RE, Twaddel W, Goloubeva OG, Wong KK et al. Metformin prevents liver tumorigenesis by inhibiting pathways driving hepatic lipogenesis. Cancer Prev Res (Phila) 2012; 5: 544–552. [PubMed: 22467080]

11. DePeralta DK, Wei L, Ghoshal S, Schmidt B, Lauwers GY, Lanuti M et al. Metformin prevents hepatocellular carcinoma development by suppressing hepatic progenitor cell activation in a rat model of cirrhosis. Cancer 2016; 122: 1216–1227. [PubMed: 26914713]

12. Tajima K, Nakamura A, Shirakawa J, Togashi Y, Orime K, Sato K et al. Metformin prevents liver tumorigenesis induced by high-fat diet in C57Bl/6 mice. Am J Physiol Endocrinol Metab 2013; 305: E987–998. [PubMed: 23964070]

13. Liu X, Liu F, Gao S, Reske J, Li A, Wu C-L et al. A single non-synonymous NCOA5 variation in type 2 diabetic patients with hepatocellular carcinoma impairs the function of NCOA5 in cell cycle regulation. Cancer Lett 2017; 391: 152–161. [PubMed: 28137631]

14. el-Deiry WS, Tokino T, Velculescu VE, Levy DB, Parsons R, Trent JM et al. WAF1, a potential mediator of p53 tumor suppression. Cell 1993; 75: 817–825. [PubMed: 8242752]

15. He GB, Dhar D, Nakagawa H, Font-Burgada J, Ogata H, Jiang YH et al. Identification of Liver Cancer Progenitors Whose Malignant Progression Depends on Autocrine IL-6 Signaling. Cell 2013; 155: 384–396. [PubMed: 24120137]

16. Luo X, Liao R, Hanley KL, Zhu HH, Malo KN, Hernandez C et al. Dual Shp2 and Pten Deficiencies Promote Non-alcoholic Steatohepatitis and Genesis of Liver Tumor-Initiating Cells. Cell Rep 2016; 17: 2979–2993. [PubMed: 27974211]

17. Finkin S, Yuan D, Stein I, Taniguchi K, Weber A, Unger K et al. Ectopic lymphoid structures function as microniches for tumor progenitor cells in hepatocellular carcinoma. Nat Immunol 2015; 16: 1235–1244. [PubMed: 26502405]

18. Yu LX, Ling Y, Wang HY. Role of nonresolving inflammation in hepatocellular carcinoma development and progression. NPJ Precis Oncol 2018; 2: 6. [PubMed: 29872724]

19. Wherry EJ, Ha SJ, Kaech SM, Haining WN, Sarkar S, Kalia V et al. Molecular signature of CD8+ T cell exhaustion during chronic viral infection. Immunity 2007; 27: 670–684. [PubMed: 17950003]

20. Zheng C, Zheng L, Yoo JK, Guo H, Zhang Y, Guo X et al. Landscape of Infiltrating T Cells in Liver Cancer Revealed by Single-Cell Sequencing. Cell 2017; 169: 1342–1356 e1316. [PubMed: 28622514]

21. Pauken KE, Sammons MA, Odorizzi PM, Manne S, Godec J, Khan O et al. Epigenetic stability of exhausted T cells limits durability of reinvigoration by PD-1 blockade. Science 2016; 354: 1160–1165. [PubMed: 27789795]

22. Lee SY, Lee SH, Yang EJ, Kim EK, Kim JK, Shin DY et al. Metformin Ameliorates Inflammatory Bowel Disease by Suppression of the STAT3 Signaling Pathway and Regulation of the between Th17/Treg Balance. PLoS One 2015; 10: e0135858. [PubMed: 26360050]

23. Tan XL, Bhattacharyya KK, Dutta SK, Bamlet WR, Rabe KG, Wang E et al. Metformin suppresses pancreatic tumor growth with inhibition of NFkappaB/STAT3 inflammatory signaling. Pancreas 2015; 44: 636–647. [PubMed: 25875801]

24. Liberzon A, Subramanian A, Pinchback R, Thorvaldsdottir H, Tamayo P, Mesirov JP. Molecular signatures database (MSigDB) 3.0. Bioinformatics 2011; 27: 1739–1740. [PubMed: 21546393]

25. Roessler S, Jia HL, Budhu A, Forgues M, Ye QH, Lee JS et al. A unique metastasis gene signature enables prediction of tumor relapse in early-stage hepatocellular carcinoma patients. Cancer Res 2010; 70: 10202–10212. [PubMed: 21159642]

26. Villanueva A, Portela A, Sayols S, Battiston C, Hoshida Y, Mendez-Gonzalez J et al. DNA methylation-based prognosis and epidrivers in hepatocellular carcinoma. Hepatology 2015; 61: 1945–1956. [PubMed: 25645722]

27. Gentles AJ, Plevritis SK, Majeti R, Alizadeh AA. Association of a leukemic stem cell gene expression signature with clinical outcomes in acute myeloid leukemia. Jama 2010; 304: 2706–2715. [PubMed: 21177505]

28. Arendt BM, Comelli EM, Ma DW, Lou W, Teterina A, Kim T et al. Altered hepatic gene expression in nonalcoholic fatty liver disease is associated with lower hepatic n-3 and n-6 polyunsaturated fatty acids. Hepatology 2015; 61: 1565–1578. [PubMed: 25581263]

29. Warfel NA, El-Deiry WS. p21WAF1 and tumourigenesis: 20 years after. Curr Opin Oncol 2013; 25: 52–58. [PubMed: 23159848]

30. Gartel AL, Tyner AL. Transcriptional regulation of the p21((WAF1/CIP1)) gene. Exp Cell Res 1999; 246: 280–289. [PubMed: 9925742]

31. Abbas T, Dutta A. p21 in cancer: intricate networks and multiple activities. Nat Rev Cancer 2009; 9: 400–414. [PubMed: 19440234]

32. Cmielova J, Rezacova M. p21Cip1/Waf1 protein and its function based on a subcellular localization [corrected]. J Cell Biochem 2011; 112: 3502–3506. [PubMed: 21815189]

33. Nguyen P, Valanejad L, Cast A, Wright M, Garcia JM, El-Serag HB et al. Elimination of Age-Associated Hepatic Steatosis and Correction of Aging Phenotype by Inhibition of cdk4-C/EBPalpha-p300 Axis. Cell Rep 2018; 24: 1597–1609. [PubMed: 30089269]

34. Tomita K, Teratani T, Suzuki T, Oshikawa T, Yokoyama H, Shimamura K et al. p53/p66Shc-mediated signaling contributes to the progression of non-alcoholic steatohepatitis in humans and mice. J Hepatol 2012; 57: 837–843. [PubMed: 22641095]

35. Wu H, Wade M, Krall L, Grisham J, Xiong Y, Van Dyke T. Targeted in vivo expression of the cyclin-dependent kinase inhibitor p21 halts hepatocyte cell-cycle progression, postnatal liver development and regeneration. Genes Dev 1996; 10: 245–260. [PubMed: 8595876]

36. Yano M, Ohkoshi S, Aoki YH, Takahashi H, Kurita S, Yamazaki K et al. Hepatitis B virus X induces cell proliferation in the hepatocarcinogenesis via up-regulation of cytoplasmic p21 expression. Liver Int 2013; 33: 1218–1229. [PubMed: 23590292]

37. Marhenke S, Buitrago-Molina LE, Endig J, Orlik J, Schweitzer N, Klett S et al. p21 promotes sustained liver regeneration and hepatocarcinogenesis in chronic cholestatic liver injury. Gut 2014; 63: 1501–1512. [PubMed: 24092862]

38. Ehedego H, Boekschoten MV, Hu W, Doler C, Haybaeck J, Gabetaler N et al. p21 ablation in liver enhances DNA damage, cholestasis, and carcinogenesis. Cancer Res 2015; 75: 1144–1155. [PubMed: 25608711]

39. Nicolae CM, O'Connor MJ, Constantin D, Moldovan GL. NFkappaB regulates p21 expression and controls DNA damage-induced leukemic differentiation. Oncogene 2018; 37: 3647–3656. [PubMed: 29622796]

40. Giovannucci E, Harlan DM, Archer MC, Bergenstal RM, Gapstur SM, Habel LA et al. Diabetes and cancer: a consensus report. Diabetes Care (Consensus Development Conference Research Support, Non-U.S. Gov't) 2010; 33: 1674–1685. [PubMed: 20587728]

41. Donadon V, Balbi M, Mas MD, Casarin P, Zanette G. Metformin and reduced risk of hepatocellular carcinoma in diabetic patients with chronic liver disease. Liver Int 2010; 30: 750–758. [PubMed: 20331505]

42. Schulte L, Scheiner B, Voigtlander T, Koch S, Schweitzer N, Marhenke S et al. Treatment with metformin is associated with a prolonged survival in patients with hepatocellular carcinoma. Liver Int 2019; 39: 714–726. [PubMed: 30663219]

43. Kalender A, Selvaraj A, Kim SY, Gulati P, Brule S, Viollet B et al. Metformin, independent of AMPK, inhibits mTORC1 in a rag GTPase-dependent manner. Cell Metab 2010; 11: 390–401. [PubMed: 20444419]

44. Algire C, Moiseeva O, Deschenes-Simard X, Amrein L, Petruccelli L, Birman E et al. Metformin reduces endogenous reactive oxygen species and associated DNA damage. Cancer Prev Res (Phila) 2012; 5: 536–543. [PubMed: 22262811]

45. Hirsch HA, Iliopoulos D, Struhl K. Metformin inhibits the inflammatory response associated with cellular transformation and cancer stem cell growth. Proc Natl Acad Sci U S A 2013; 110: 972–977. [PubMed: 23277563]

46. Fujita K, Iwama H, Miyoshi H, Tani J, Oura K, Tadokoro T et al. Diabetes mellitus and metformin in hepatocellular carcinoma. World journal of gastroenterology (Review) 2016; 22: 6100–6113. [PubMed: 27468203]

47. Molnar Z, Millward AB, Tse W, Demaine AG. p21(WAF1/CIP1) Expression is Differentially Regulated by Metformin and Rapamycin. Int J Chronic Dis 2014; 2014: 327640. [PubMed: 26464852]

48. Noren Hooten N, Martin-Montalvo A, Dluzen DF, Zhang Y, Bernier M, Zonderman AB et al. Metformin-mediated increase in DICER1 regulates microRNA expression and cellular senescence. Aging Cell 2016; 15: 572–581. [PubMed: 26990999]

49. Rohr-Udilova N, Klinglmuller F, Schulte-Hermann R, Stift J, Herac M, Salzmann M et al. Deviations of the immune cell landscape between healthy liver and hepatocellular carcinoma. Sci Rep 2018; 8: 6220. [PubMed: 29670256]

50. Eikawa S, Nishida M, Mizukami S, Yamazaki C, Nakayama E, Udono H. Immune-mediated antitumor effect by type 2 diabetes drug, metformin. Proc Natl Acad Sci U S A 2015; 112: 1809–1814. [PubMed: 25624476]
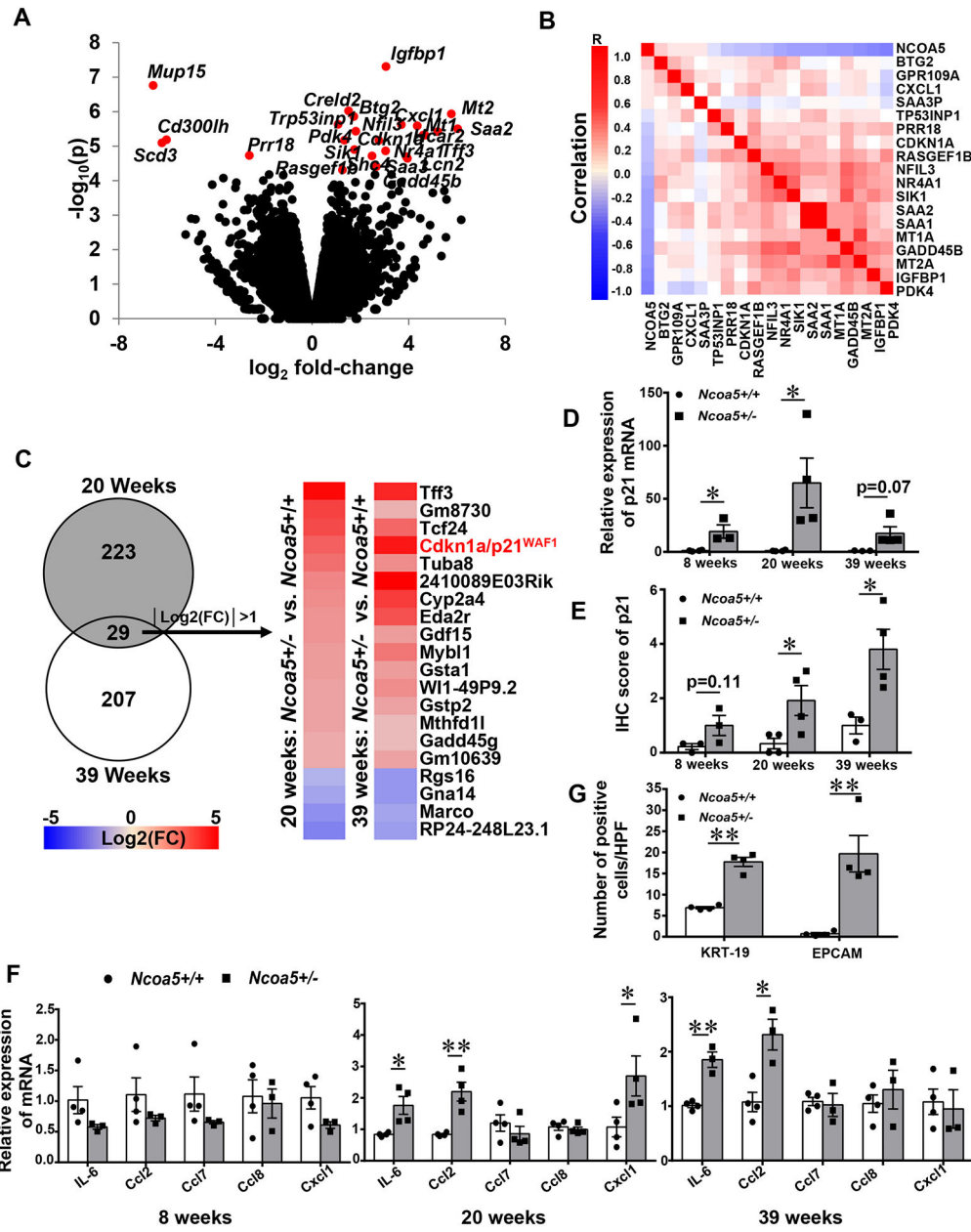
51. Shalapour S, Lin XJ, Bastian IN, Brain J, Burt AD, Aksenov AA et al. Erratum: Inflammation-induced IgA(+) cells dismantle anti-liver cancer immunity. Nature 2017; 551: 340–345. [PubMed: 29144460]

52. Verdura S, Cuyas E, Martin-Castillo B, Menendez JA. Metformin as an archetype immuno-metabolic adjuvant for cancer immunotherapy. Oncoimmunology 2019; 8: e1633235. [PubMed: 31646077]

Figure 1. Dysregulated genes expression and increased putative HPCs in Preneoplastic Livers of *Ncoa5*^{+/−} Male Mouse.

(A) Volcano plot showing EdgeR differential expression analysis results from 20-week-old male *Ncoa5*^{+/−} vs. *Ncoa5*^{+/+} mouse liver RNA sequencing (n=4). Genes with significant changes in expression (FDR<0.05) are red and labeled with the gene name. (B) Correlation heatmap of significant human homologs of differentially expressed murine genes vs. *NCOA5* expression in HCC tumors and adjacent tissues (TCGA-LIHC data). (C) Differentially expressed genes in *Ncoa5*^{+/−} vs *Ncoa5*^{+/+} liver tissue identified in both 20- and 39-week- old cohorts (FDR<0.05). Among 29 genes common to both groups, 20 of them are with an absolute value of log2 fold change > 1 in a similarly altered direction. (D) The mRNA levels of p21[WAF1/CIP1] in the liver of *Ncoa5*^{+/−} vs *Ncoa5*^{+/+} male mice (n=4 per

group, except for 8-week-old $Ncoa5^{+/-}$ and 39-week-old $Ncoa5^{+/+}$ mice n=3) at indicated ages by using qPCR analysis. (E) Quantifications of IHC staining of p21$^{WAF1/CIP1}$ in the liver of $Ncoa5^{+/-}$ and $Ncoa5^{+/+}$ male mice at indicated ages. n=3 for 8-week old mice, n=4 for 20-week-old mice, n=3 or 4 for 39-week-old $Ncoa5^{+/-}$ or $Ncoa5^{+/+}$ mice, respectively. (F) The mRNA level of several cytokines and chemokines in the liver of $Ncoa5^{+/-}$ and $Ncoa5^{+/+}$ male mice at indicated ages. For 8-week-old and 39-week-old mice, n=3 or 4 for $Ncoa5^{+/-}$ or $Ncoa5^{+/+}$ mice, respectively. For 20-week-old mice n=4 for both groups. (G) Quantification of KRT-19- or EPCAM-positive HPC-like cell in the liver of 20-week-old $Ncoa5^{+/-}$ and $Ncoa5^{+/+}$ male mice (n=4 per group). All data represented as mean± SEM. Statistical significance was determined by unpaired two-tail t-test. * p<0.05; ** p<0.01.
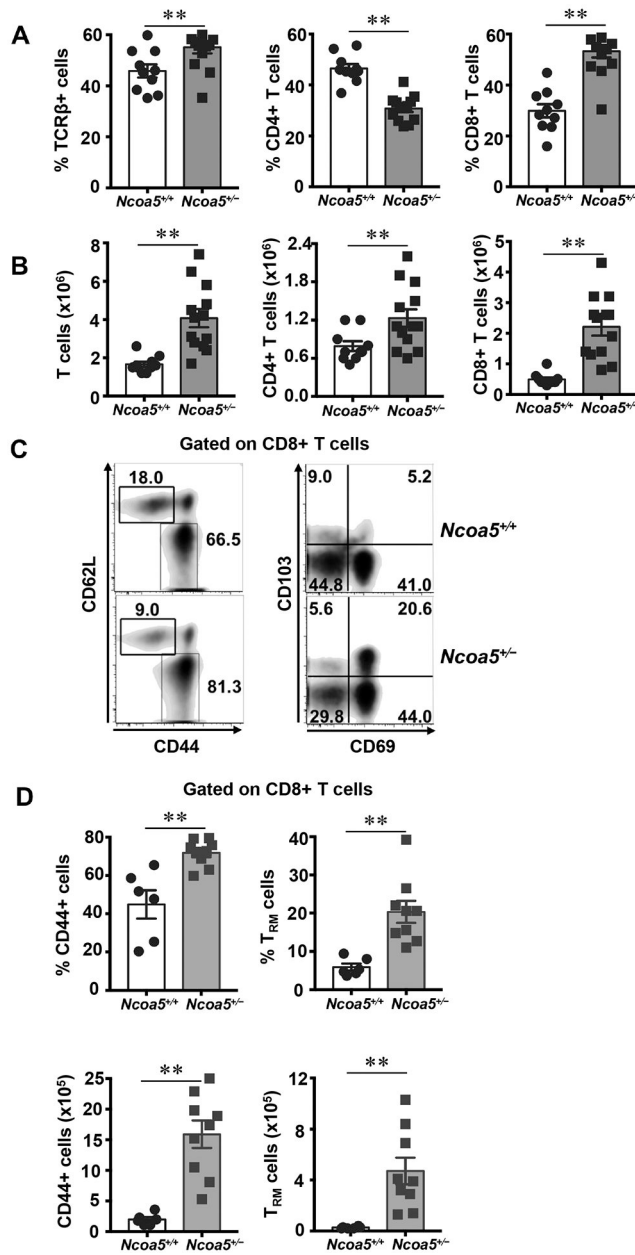
Figure 2. Frequency, absolute numbers and subsets of CD8+ T cells in livers of *Ncoa5*$^{+/-}$ mice.
(A) Percentages and (B) absolute numbers of the T lymphocytes in the livers of *Ncoa5*$^{+/+}$ and *Ncoa5*$^{+/-}$ mice. Data in A and B are pooled from 5 independent experiments with a total of *Ncoa5*$^{+/+}$ (n=10) and *Ncoa5*$^{+/-}$ (n=13) mice at the age of 8–10 months analyzed in each cohort. (C) Representative density plots showing the percentages of naive (CD62L+CD44−), activated (CD62L− CD44+) and tissue resident memory (CD103+CD69+) CD8+ cells in the livers of *Ncoa5*$^{+/+}$ (top) and *Ncoa5*$^{+/-}$ (bottom) mice. (D) Percentages (top) and absolute numbers (bottom) of the subsets of CD8+ T cells in the livers of *Ncoa5*$^{+/+}$ and *Ncoa5*$^{+/-}$ mice. Data in C, D are pooled from 3 independent experiments with a total of *Ncoa5*$^{+/+}$ (n=6) and *Ncoa5*$^{+/-}$ (n=9) mice at the age of 8–10 months. Error bars represent SEM.
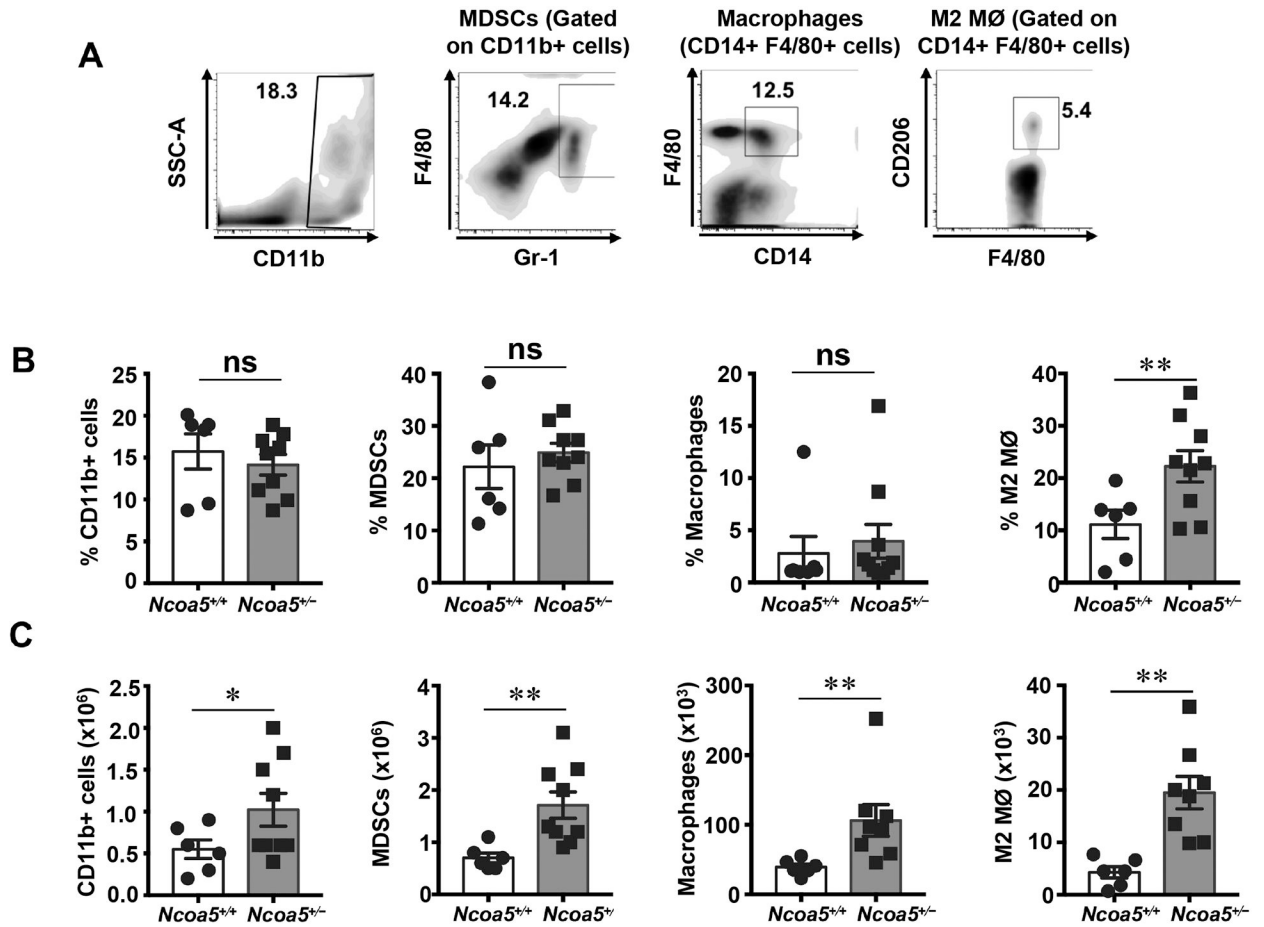
Statistical significance was determined by unpaired two-tail t-test. * p < 0.05, ** p < 0.01, ns: not significant.

Figure 3. Frequency and Absolute numbers of MDSCs, macrophages and M2 macrophages in livers of *Ncoa5*$^{+/-}$ mice.

(A) Representative density plots showing the gating strategy for the various myeloid populations, as indicated. (B) Percentages (C) and absolute numbers of the total CD11b+, MDSCs (CD11b+F4/80+Gr-1+), macrophages (CD14+F4/80+) and M2 macrophages (CD14+F4/80+ CD206+) in the livers of *Ncoa5*$^{+/+}$ and *Ncoa5*$^{+/-}$ mice. Data in B, C are pooled from 3 independent experiments with a total of *Ncoa5*$^{+/+}$ (n=6) and *Ncoa5*$^{+/-}$ (n=9) mice at the age of 8–10 months analyzed in each cohort. Error bars represent SEM. Statistical significance was determined by unpaired two-tail t-test. * p < 0.05, ** p < 0.01, ns: not significant.
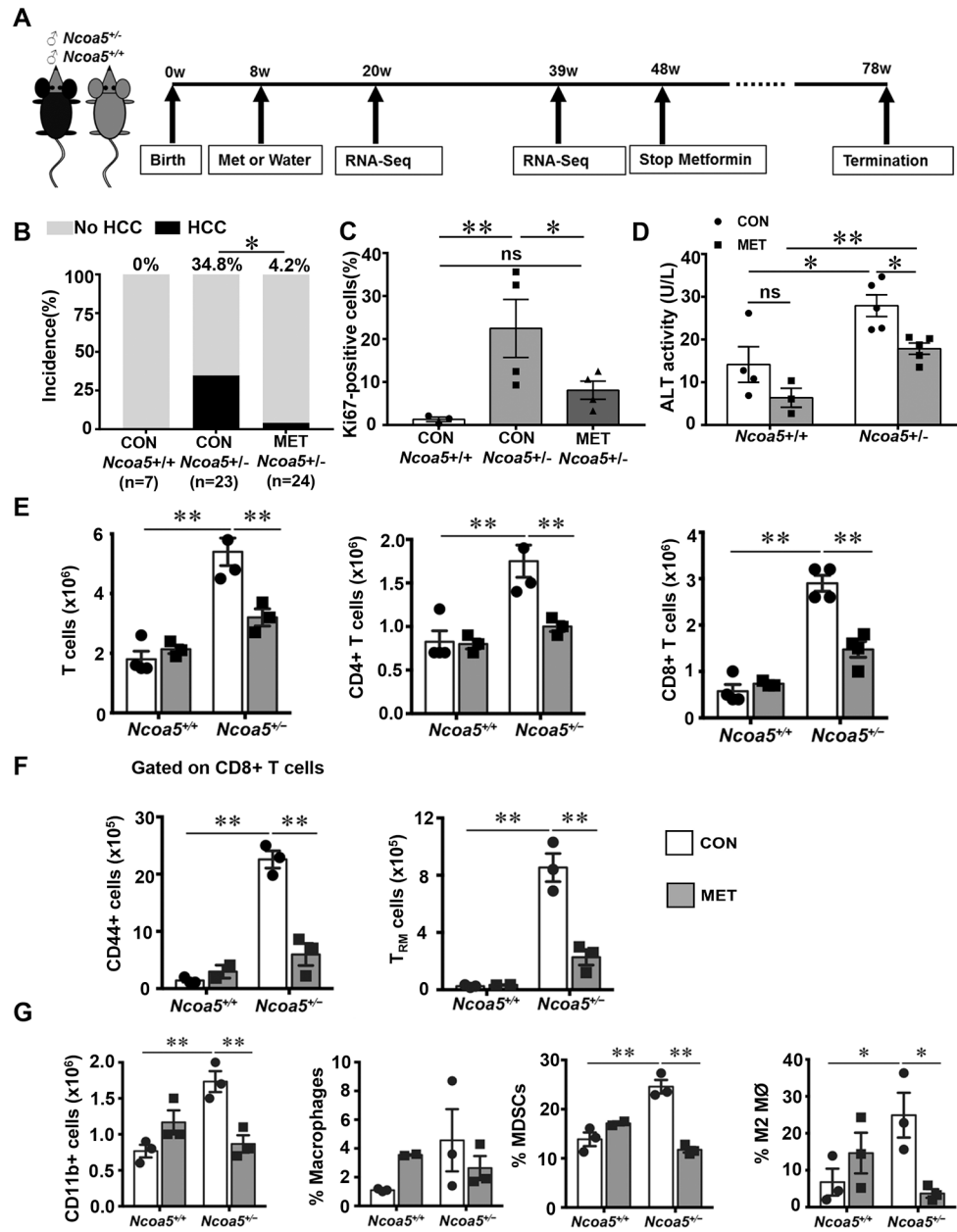
Figure 4. Effects of Metformin on the characteristics of precancerous livers and HCC Incidence in *Ncoa5*$^{+/-}$ Male mice.

(A) Schematic diagram showing the experimental set. Arrows indicate the age of mice administrated procedures as indicated. (B) Percent HCC incidence in *Ncoa5*$^{+/-}$ male mice at 78 weeks of age treated with (MET) or without metformin (CON). Fisher's Exact Test was used to determine significance. (C) Quantification of IHC staining of Ki67 in livers derived from 39-week-old *Ncoa5*$^{+/+}$ and *Ncoa5*$^{+/-}$ male mice (n=4 per group, except for metformin untreated *Ncoa5*$^{+/+}$ mice n=3) with or without metformin treatment. (D) Serum alanine aminotransferase (ALT) activity in 39-week-old male mice as indicated. n=3 for metformin treated or untreated *Ncoa5*$^{+/+}$ mice. n=4 for metformin treated or untreated *Ncoa5*$^{+/-}$ mice. (E, F) Absolute numbers of total T, CD4+ T and CD8+ T cells (E), activated and resident

memory CD8+ T cells (F) in the livers of $Ncoa5^{+/+}$ and $Ncoa5^{+/-}$ mice untreated or treated with metformin. Data in E and F are from $Ncoa5^{+/+}$ and $Ncoa5^{+/-}$ metformin untreated or treated mice at the age of 11–14 months. n=3 mice for each group in (E) except that n=4 for untreated $Ncoa5^{+/-}$ mice. n=3 mice for each group in (F) for $Ncoa5^{+/+}$ mice treated with or without metformin, except that n=2 for metformin treated $Ncoa5^{+/+}$ mice. (G) Absolute number of myeloid cell and the percentage of its subsets including macrophages (CD14+F4/80+), MDSCs (CD11b+F4/80+Gr-1+), and M2 macrophages (CD14+F4/80+CD206+) in the livers of $Ncoa5^{+/+}$ and $Ncoa5^{+/-}$ mice untreated or treated with metformin. Data in G are from 2 independent experiments in which n=3 mice per group, except that n=2 for metformin treated $Ncoa5^{+/+}$ mice for macrophage and MDSCs counting. SEMs were calculated and drawn for the two-sample group; however, no statistical test was carried out using this group. Error bars represent SEM. Statistical significance was determined by two-way ANOVA. * $p < 0.05$, ** $p < 0.01$, ns: not significant.
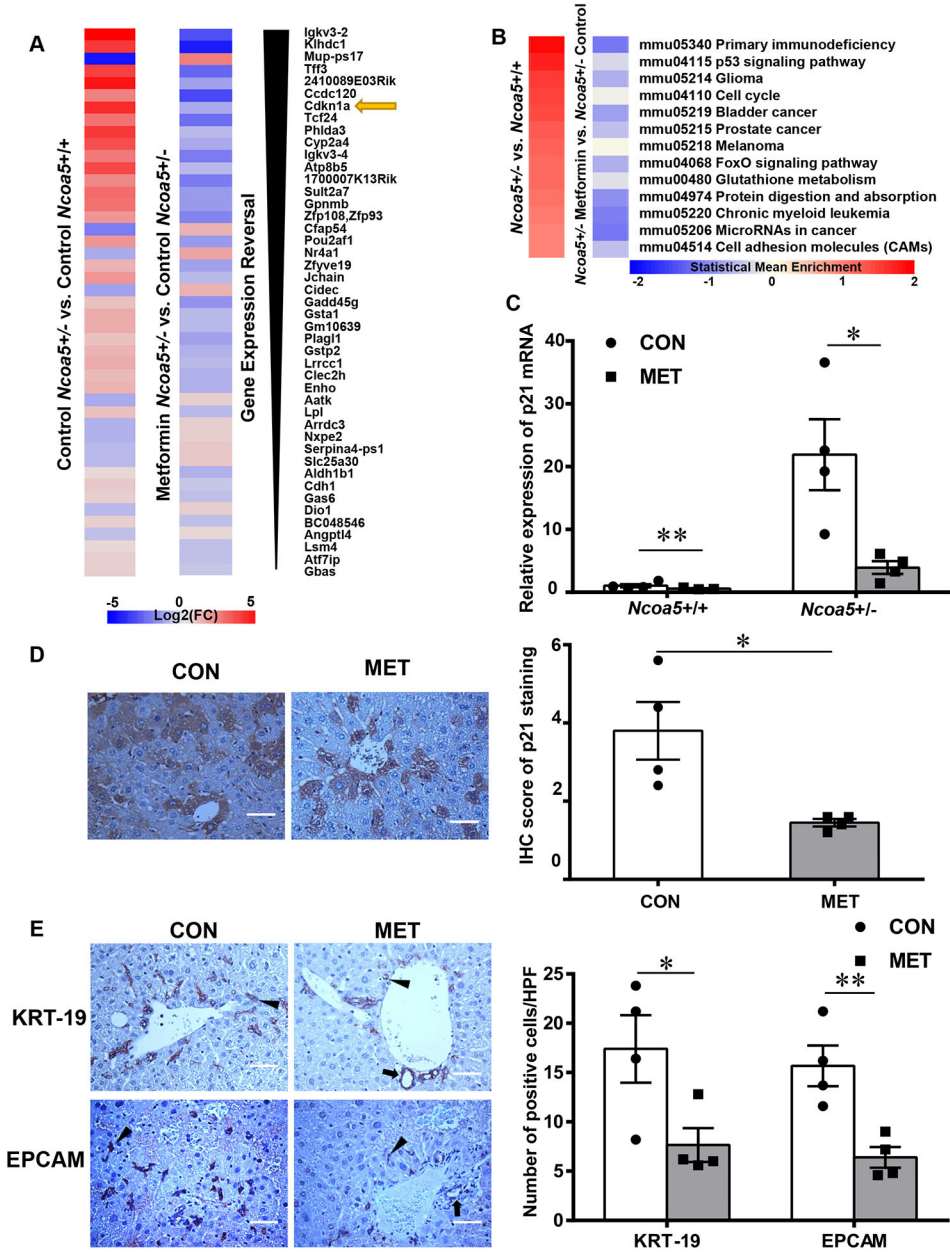
Figure 5. Effects of metformin on Dysregulated Genes, Cytoplasmic-p21$^{WAF1/CIP1}$-Positive Hepatocytes and HPCs in $Ncoa5^{+/-}$ Male Mouse Liver.

(A) Differentially up- (red) or down- (blue) expressed genes between two experimental groups as indicated. 46 genes, whose expression were altered in 39-week-old $Ncoa5^{+/-}$ vs $Ncoa5^{+/+}$ male mouse livers, were reversed by metformin treatment as determined by Cuffdiff (Log2 fold change as indicated, FDR<0.05). (B) KEGG pathways with up-regulated (FDR<0.25) expression in 39-week-old $Ncoa5^{+/-}$ vs $Ncoa5^{+/+}$ male mouse livers that exhibited a reversed trend with metformin treatment as determined by GAGE. (C) The mRNA levels of p21$^{WAF1/CIP1}$ in the livers of 39-week-old male mice with or without metformin treatment tested by using RT-QPCR analysis. n=4 for each group except for metformin treated $Ncoa5^{+/+}$ mice. n=3. (D) Representative images and quantifications of

IHC staining of p21$^{\text{WAF1/CIP1}}$ on the liver sections derived from 39-week-old *Ncoa5*$^{+/-}$ male mice (n=4 per group). Scale bar, 50 μm. (E) Representative images and quantifications of IHC staining of KRT-19 or EPCAM on the liver sections derived from 39-week-old *Ncoa5*$^{+/-}$ male mice treated with or without metformin (n=4 per group). Interlobular bile ducts (arrow) were excluded from the counting, while the other KRT-19- or EPCAM-positively stained cells (arrowhead) were counted as putative HPCs. Scale bar, 50 μm. All data represented as mean± SEM. Statistical significance was determined by unpaired two-tailed t-test. * p<0.05; ** p<0.01.
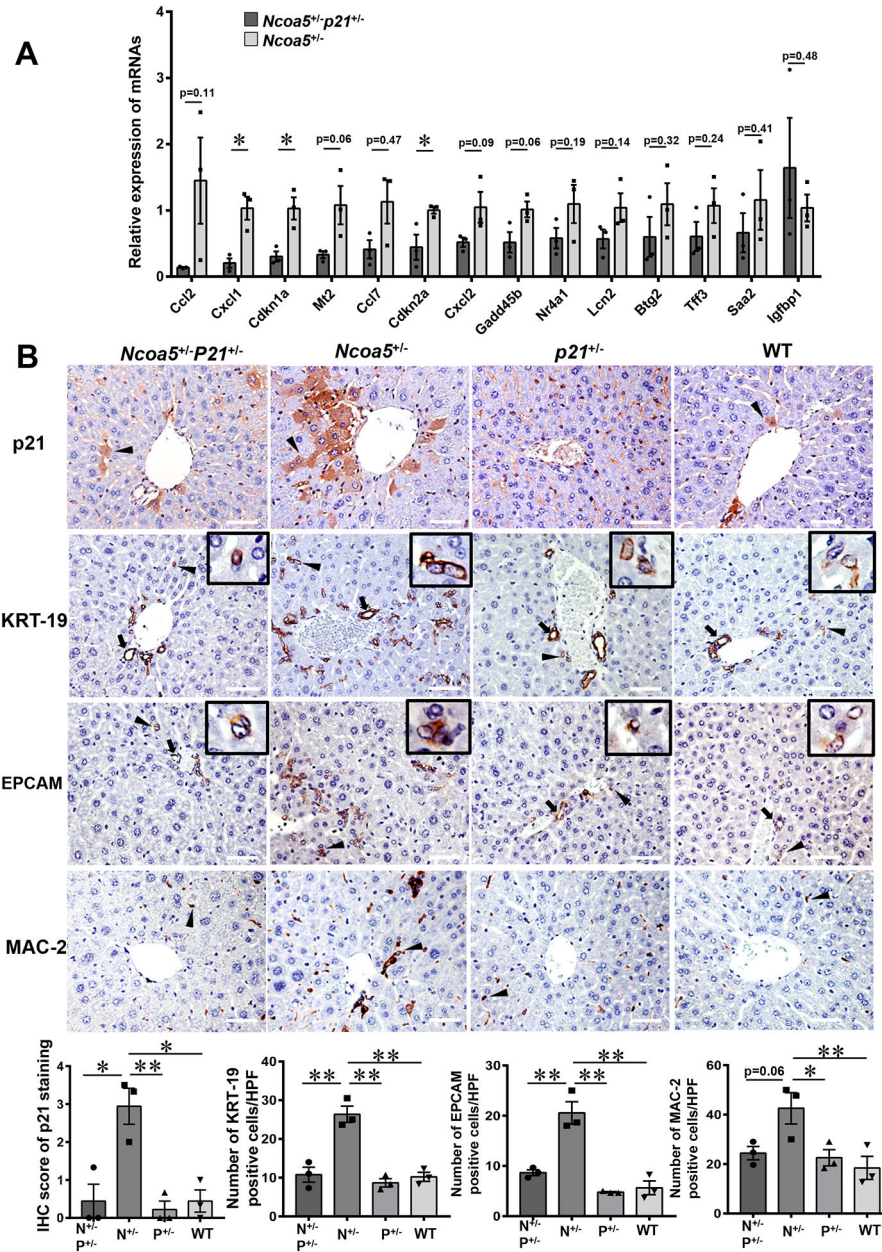
Figure 6. Effect of heterozygous deletion of *p21* gene on the livers of *Ncoa5*^{+/−} male mice.
(A) Quantitative RT-PCR analysis of 14 genes in livers of *Ncoa5*^{+/−}*p21*^{+/−} and *Ncoa5*^{+/−} mice at age of 20 weeks using TaqMan Custom Array. These 14 genes were identified as the early up-regulated genes in livers of *Ncoa5*^{+/−} mice (Fig. 1 and Supplementary Fig. S1). (B) Representative images and quantifications of IHC staining of p21[WAF1/CIP1], KRT-19, EPCAM and MAC-2 on liver sections derived from 20-week-old *Ncoa5*^{+/−}*p21*^{+/−} and *Ncoa5*^{+/−} male mice (n=3). Interlobular bile ducts (arrow) were excluded from the counting, while the other KRT-19- or EPCAM-positively stained cells (arrowhead) were counted as putative HPCs. Inset shows detail of putative KRT-19- or EPCAM-positive cells. Arrowhead in images of IHC staining of MAC-2 indicated MAC-2 positive cells. All data represented as

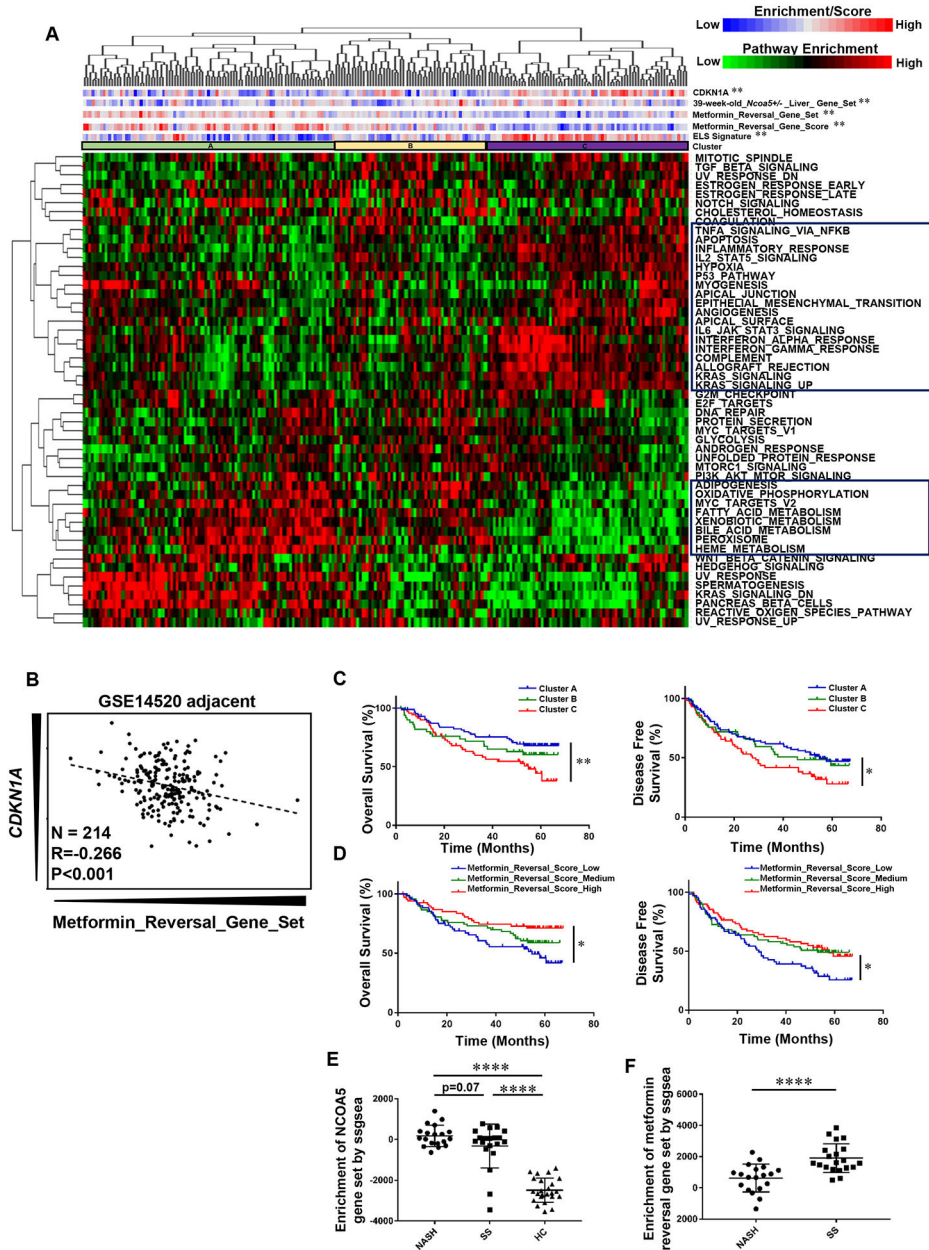mean± SEM. Statistical significance was determined by unpaired two-tailed t-test. * p<0.05, ** p<0.01.

Figure 7. Association of CDKN1A/p21^{WAF1/CIP1} expression and Ncoa5 gene set with HCC Patients and NASH patients.

(A) Heatmap showing three distinct subgroups of HCC patients identified by unsupervised clustering analysis of Hallmark gene sets in the adjacent noncancerous liver tissues from HCC patients (GSE14520, n=214). Indicated gene and gene sets are displayed for each sample. The NCOA5 gene set was created by converting the genes found differentially expressed in livers of 39-week-old $Ncoa5^{+/-}$ mice compared with age-matched $Ncoa5^{+/+}$ mice by RNA-Seq analysis to human homologs in human HCC samples dataset (GSE14520). Metformin reversal gene set was derived by converting the genes found differentially expressed in livers of 39-week-old $Ncoa5^{+/-}$ mice but then reversed in metformin treated $Ncoa5^{+/-}$ mice to human homologs. Metformin reversal gene score for

individual HCC patients was defined as the weighted sum of this patient's gene expression values for genes from the metformin reversal gene set as described previously [27]. The weight of genes was calculated based on the comparison of gene expression profiles from untreated $Ncoa5^{+/+}$, untreated $Ncoa5^{+/-}$ and metformin treated $Ncoa5^{+/-}$ mouse livers. (B) A regression coefficients graph showing a negative correlation between CDKN1A/p21$^{WAF1/CIP1}$ expression and enrichment of metformin reversal gene set in the adjacent noncancerous liver tissues. (C) Kaplan-Meier survival analysis of OS (left) or DFS (right) for three subgroups of HCC patients. (D) Kaplan-Meier survival analysis of OS (left) or DFS (right) between patients with high, medium and low metformin reversal gene score in their adjacent noncancerous liver tissues. The differences between indicated two curves were determined by two-sided log-rank tests. * p<0.05; ** p<0.01. (E,F) Enrichment of NCOA5 Gene Set (E) and Metformin Reversal Gene Set (F) assessed by ssGSEAProjection for liver samples (GSE89632), from NASH patients (n=19), simple steatosis (SS) patients (n=20) and healthy control (HC, n=24). Statistical significance was determined by unpaired two-tailed t-test. ****p<0.0001.